Special Double Issue Article

Yu Zhao*, Jue Wang, Scott Huxtable, Giti A. Khodaparast and Shashank Priya

Role of Sintering Atmosphere and Synthesis Parameters on Electrical Conductivity of ZnO

Abstract: ZnO-based compositions are of great interest for high-temperature thermoelectric applications. In this study, *n*-type Al-doped ZnO was sintered under varying atmospheres and the changes in electrical conductivity along with chemical defects were analyzed. The electrical conductivity of Al-doped ZnO (ZnO-Al) exhibited large variation from 10^{-5} to 10^{3} S/cm as the sintering atmosphere was changed from air to nitrogen to vacuum. The low oxygen partial pressure assisted Al substitution in ZnO and increased the interstitial Zn, which increased the carrier concentration and improved the electrical conductivity. Using vacuum sintering, the electrical conductivity of ZnO was enhanced as the concentration of Al doping was increased from 1 to 3 at.%. Two sets of starting powders were used for sintering studies, one synthesized through the ball-milling and other through the sol–gel chemical synthesis. It was found that the Al substitution is improved by using chemically synthesized ZnO-Al powders.

Keywords: electrical conductivity, ZnO, sintering atmosphere, chemical defect, doping, thermoelectric

DOI 10.1515/ehs-2015-0002

Introduction

ZnO is a promising thermoelectric material due to its combination of good Seebeck coefficient (around –200 μV/K) and excellent stability at high temperature (Özgür et al. 2005; Ohtaki, Tsubota, and Eguchi 1996; Ong, Singh, and Wu 2011). It is a natural *n*-type wide-band gap semiconductor because of the slight deviation from stoichiometry (Özgür et al. 2005) that occurs during synthesis. Similar to other oxide thermoelectric materials, relatively low carrier concentration limits its potential to achieve higher figure of merit. Experimental and theoretical value of mobility (μ) in ZnO has been found to be quite high in comparison with other oxide-type materials; however, the carrier concentration (n) needs to be further increased in order to improve the electrical conductivity (σ) (Özgür et al. 2005).

Doping and sintering conditions can modify the defect chemistry and thereby influence the electrical behavior of ZnO. Aluminum is a common dopant utilized for ZnO, and previous studies have revealed that σ of Al_2O_3-modified ZnO can be increased by more than three orders of magnitude (Ohtaki, Tsubota, and Eguchi 1996; Tsubota et al. 1997). Electrical conductivity enhancement has been primarily attributed to the Al^{3+} substitution on the Zn^{2+} site resulting in a free electron (Cai et al. 2003). However, the doping concentration is restricted due to the limited Al solubility in ZnO with a maximum of 0.3 at.% at 1,400°C (Shirouzu et al. 2007). Additional Al_2O_3 forms the secondary phase corresponding to $ZnAl_2O_4$, which has a negative impact on the magnitude of electrical conductivity (Cai et al. 2003; Zhao et al. 2014). According to phase diagram of the Al_2O_3–ZnO system, the reaction between ZnO and Al_2O_3 varies considerably with temperature, which changes the function of Al in ZnO matrix. Studies have shown that the Al_2O_3-doped ZnO sintered at 1,400°C exhibits much better σ value than at lower temperatures, such as 1,100°C (Zhao et al. 2014; Han, Mantas, and Senos 2001). Relatively low sintering temperature is required (Jood et al. 2011; Zhao et al. 2012) to achieve low thermal conductivity in nanostructured ZnO, but that low temperature will also lower the carrier concentration and hence electrical conductivity. Thus, a better synthesis approach is required in order to sinter bulk ZnO with higher carrier concentration at low temperatures.

***Corresponding author: Yu Zhao,** Bio-Inspired Materials and Devices Laboratory (BMDL), Center for Energy Harvesting Materials and Systems (CEHMS), Virginia Tech, Blacksburg, VA 24061, USA, E-mail: zhaoyu@vt.edu
Jue Wang: E-mail: jue12@vt.edu, **Scott Huxtable:** E-mail: huxtable@vt.edu, Bio-Inspired Materials and Devices Laboratory (BMDL), Center for Energy Harvesting Materials and Systems (CEHMS), Virginia Tech, Blacksburg, VA 24061, USA
Giti A. Khodaparast, Physics Department, Virginia Tech, Blacksburg, VA 24061, USA, E-mail: khoda@vt.edu
Shashank Priya, Bio-Inspired Materials and Devices Laboratory (BMDL), Center for Energy Harvesting Materials and Systems (CEHMS), Virginia Tech, Blacksburg, VA 24061, USA, E-mail: spriya@vt.edu

The sintering atmosphere is another important variable that can be used to control the electrical properties of ZnO. Bérardan (2010) have shown that Al-doped ZnO samples sintered in nitrogen ambient have larger σ than those sintered in air ambient. This behavior was attributed to the oxygen vacancy formation. The difference in σ could be explained by the change of carrier density, which is greatly influenced by the surrounding atmosphere, especially the oxygen concentration. One important reason for lowering the carrier density is the formation of electron compensator Zn^{2+} vacancy whose formation requires oxygen (Zhao et al. 2014). On the other hand, it is intuitive that partial pressure of oxygen might impact the nature of Al substitution. Therefore, a comprehensive study was conducted to investigate the influence of sintering atmosphere on the electrical conductivity of ZnO.

Experimental Methods

Two types of powders with different initial physical conditions were used for synthesis. One set of starting powders was obtained using nano-sized precursor powders of ZnO (~30 nm, purity > 99.7%, Advanced Materials, LLC) and Al_2O_3 (40–50 nm, purity > 99.5%, Alfa Aesar) by ball milling for 48 h. For better Al distribution in the ZnO matrix, the second set of starting powders was synthesized by sol–gel chemical process. The chemical synthesis utilized zinc nitrate hydrate [$Zn(NO_3)_2{\cdot}6H_2O$] and aluminum nitrate hydrate [$Al(NO_3)_3{\cdot}9H_2O$] as dopants (1, 2 and 3 mol%), oxalic acid [$(COOH)_2{\cdot}2H_2O$] as a precursor and ethanol as a solvent. A viscous white gel was formed from the mixture of these organics which was stored at ambient temperature for 24 h and then dried at 80°C for 12 h. The dry gel product was calcined at 600°C for 2 h under nitrogen atmosphere to form the nano-sized ZnO-Al powders.

Ball-milled ZnO-2%Al (composition: $Zn_{0.98}Al_{0.02}O$) powders (hereafter termed as BM-ZnO-2%Al) were pressed in disk shape followed by cold isostatic pressing at 200 MPa and then sintered at 1,400°C under air or nitrogen for 5 h. ZnO-2%Al powders obtained using chemical synthesis (hereafter termed as CS-ZnO-2%Al) followed the same cold isostatic pressing method and were sintered at a different temperature (1,200°C) for 5 h under four different sintering atmospheres: air, nitrogen, 1.33 Pa (10^{-2} Torr) and 1.33×10^{-3} Pa (10^{-5} Torr). CS-ZnO-x%Al ($x = 1, 2, 3$) powders were pressed using the same process and sintered at 1,200°C for 5 h under 1.33×10^{-3} Pa (10^{-2} Torr). In order to compare the possible effects of the initial physical condition of different starting powders, pellets pressed using both BM- and CS-ZnO-2%Al powders were sintered at 1,400°C under nitrogen for 5 h. The phase(s) and microstructure of the samples were examined using X-ray diffraction (XRD, PANalytical X'Pert, CuKa; Philips, Almelo, The Netherlands) and scanning electron microscopy (SEM, LEO (Zeiss) 1550 field emission). The Oxford INCA Energy E2H X-ray energy-dispersive spectrometer (EDS) system with silicon-drifted detector was utilized for elemental analysis. Electrical conductivity was measured with the Van der Pauw method, using a Keithley 6220 as the precision current source (100 fA resolution) and a 6½ digit Keithley 2182A nano-voltmeter whose sensitivity was 10 nV. The Hall measurements were conducted in the Van der Pauw geometry to determine the carrier density. A UV-Vis-NIR spectrophotometer (Hitachi U 4100) was used for absorbance measurements on both ZnO-2%Al powders.

Results and Discussion

The XRD diffractogram of BM-ZnO-2%Al sintered under air and nitrogen atmosphere at 1,400°C is shown in Figure 1(a). Both patterns show the formation of a hexagonal wurtzite-type ZnO phase and a small fraction of the gahnite phase, $ZnAl_2O_4$ (marked with an arrow). Figure 1(b) and (c)

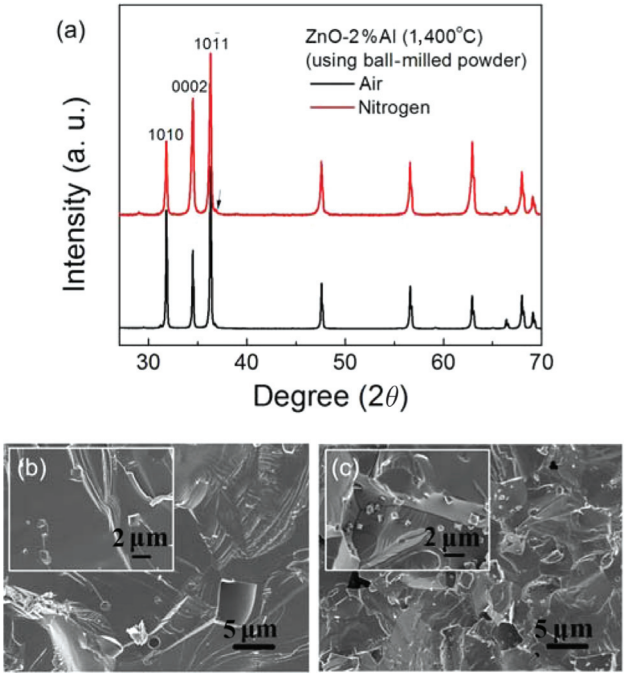

Figure 1: (a) XRD pattern of BM-ZnO-2%Al sintered under air and nitrogen atmosphere at 1,400°C; SEM micrographs (cross section) of BM-ZnO-2%Al pellets sintered at 1,400°C under (b) air and (c) nitrogen. Insets are higher magnification images showing secondary-phase precipitates.

represents the SEM images of a cross section of BM-ZnO-2%Al pellets. Both samples show dense microstructure with a small amount of second-phase precipitates that are more clearly represented in the insets of Figure 1(b) and (c). The sizes of secondary-phase precipitates were similar in the samples sintered under air and nitrogen. The grain size of ZnO sintered under nitrogen was smaller (about 10 μm) than that sintered under air (above 20 μm). Several previous studies have revealed that the zinc diffusion is responsible for the solid-state sintering (Norris et al. 1963; Gupta et al. 1968; Lee et al. 1959) since the oxygen diffusion coefficient is several orders of magnitude slower than that of zinc (Gupta et al. 1968). The oxygen from the atmosphere can diffuse faster along the grain boundaries at high temperatures and react with zinc during sintering (Gupta et al. 1968). Hence under air atmosphere the rate of ZnO sintering and grain growth is faster as compared to that under low oxygen partial pressure condition.

Figure 2 shows the electrical conductivity of the samples described in Figure 1. The electrical conductivity of ZnO-2%Al prepared in nitrogen atmosphere is about an order of magnitude greater than when it is sintered in air. The conductivity was found to increase slowly with measurement temperature. In the solid-state reaction of ZnO and Al_2O_3 during sintering, there are two most likely reactions, namely, Al^{3+} substitution on Zn^{2+} and Al^{3+} forming the gahnite phase (Cai et al. 2003; Bérardan 2010; Singh 2004; Zhan et al. 2011). In atmosphere with sufficient oxygen, the reactions can be expressed as:

$$Al_2O_3 \xrightarrow{ZnO} 2Al_{Zn}^{\cdot} + 2e' + 2O_o^{\times} + \frac{1}{2}O_2 \quad [1]$$

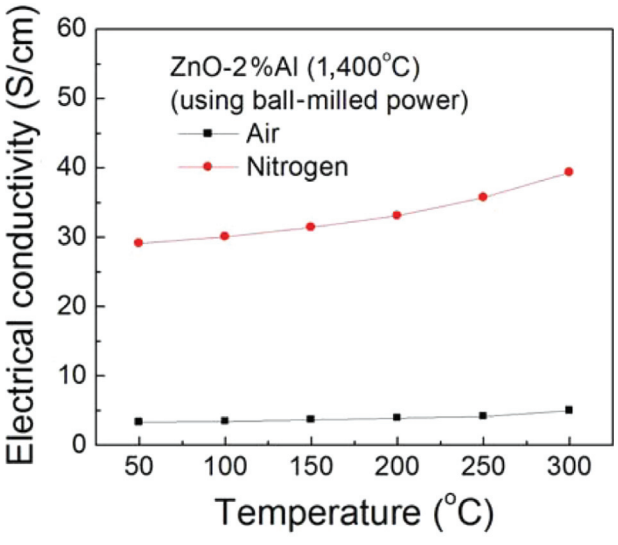

Figure 2: Electrical conductivity of BM-ZnO-2%Al sintered at 1,400°C under air and nitrogen, as a function of measurement temperature.

$$Al_2O_3 + \left(Zn_{Zn}^{\times} + 2e' + \frac{1}{2}O_2\right)_{ZnO} \xrightarrow{O_2} ZnAl_2O_4 + (V_{Zn}'')_{ZnO} \quad [2]$$

One of the byproducts of the Al_2O_3 substitution reaction is oxygen. Based on the Le Chatelier principle (Joos et al. 1991), the lack of oxygen helps the reaction [1] move forward, which can increase the amount of Al as a dopant in ZnO leading to an increase in the concentration of free carriers. According to reaction [2], Zn vacancies are more likely to appear in the presence of oxygen. The zinc vacancies can compensate for the free electrons and then lead to lower electrical conductivity (Willander et al. 2010; Wang et al. 2009). Therefore, the nitrogen atmosphere improves the electrical conductivity of ZnO by impeding the zinc vacancy formation. Further, there is a higher concentration of interstitial zinc defects in ZnO sintered under nitrogen than that sintered under air which plays the role of an electron donor (Willander et al. 2010).

The electrical conductivity for ZnO sintered under nitrogen atmosphere is about ten times greater than when it is sintered in air; however, the magnitude is still low in comparison to good thermoelectric alloys (about 10^3 S/cm). Also the high sintering temperature (1,400°C) is not good for thermal conductivity reduction. Chemically synthesized ZnO-Al powders could be one possible solution to achieve higher doping concentration at relatively low sintering temperature and thereby providing a further boost in the electrical conductivity. In a comparative experiment, the sol–gel-synthesized ZnO-Al powder compacts were sintered at a lower temperature of 1,200°C under different atmospheres: air, nitrogen, 1.33 Pa (10^{-2} Torr) and 1.33×10^{-3} Pa (10^{-5} Torr). The XRD diffractogram of this group is shown in Figure 3(a). All the XRD patterns confirm the formation of ZnO phase and a small fraction of $ZnAl_2O_4$ phase. Figure 3(b)—(e) represents the SEM images of the pellets' cross sections showing porous structures and the grain size distribution. For samples prepared in air, ZnO had grains around 5 μm with closed pores of less than 1 μm located in the corner of grains. On the other hand, the structure of the sample prepared in nitrogen was slightly more porous than the one sintered in air and some pores exhibited long rod shapes. The ZnO-2%Al samples sintered under vacuum conditions (10^{-2} and 10^{-5} Torr) exhibited porous structures (about 70% relative density), which is likely to result from the dominant vapor transport mechanism for grain growth under vacuum conditions (Zhao, Chen, Miner, and Priya 2014). The structures consist of 5–10 μm grains interspersed by nanoprecipitates. Both the grain size and the pore size of ZnO-2%Al sintered under

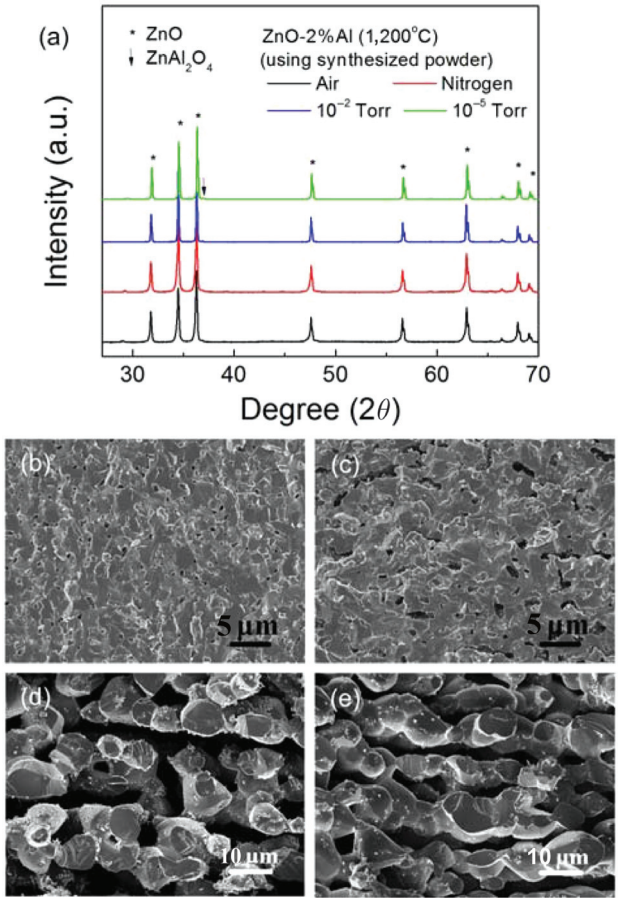

Figure 3: (a) XRD pattern of CS-ZnO-2%Al sintered under different atmospheres. SEM micrographs (cross section) of CS-ZnO-2%Al sintered at 1,200°C under (b) air, (c) nitrogen, (d) 1.33 Pa (10^{-2} Torr) and (e) 1.33×10^{-3} Pa (10^{-5} Torr).

vacuum were larger than that of the sample sintered under air and nitrogen.

Figure 4 shows the electrical conductivity of CS-ZnO-2%Al samples under different atmospheres. It can be seen that the sample sintered under air exhibited very low electrical conductivity on the order of 10^{-5} S/cm. The σ of CS-ZnO-2%Al sintered under nitrogen was 480 S/cm at 50°C and decreased to 380 S/cm at 300°C. Comparing CS-ZnO-2%Al sintered under air and nitrogen, the sample prepared in nitrogen atmosphere exhibits a tremendous improvement in electrical conductivity (seven orders of magnitude). The electrical conductivity of the CS-ZnO-2%Al was larger in comparison to BM-ZnO-2%Al sintered under the same nitrogen atmosphere (Figure 2), even though the later one used a higher sintering temperature of 1,400°C. The lower sintering temperature of 1,200°C reduces the substitution of Al^{3+} ions in ZnO matrix (Zhao et al. 2014). The CS-ZnO-2%Al pellets sintered under vacuum conditions of 1.33 Pa (10^{-2} Torr) and 1.33×10^{-3} Pa (10^{-5}

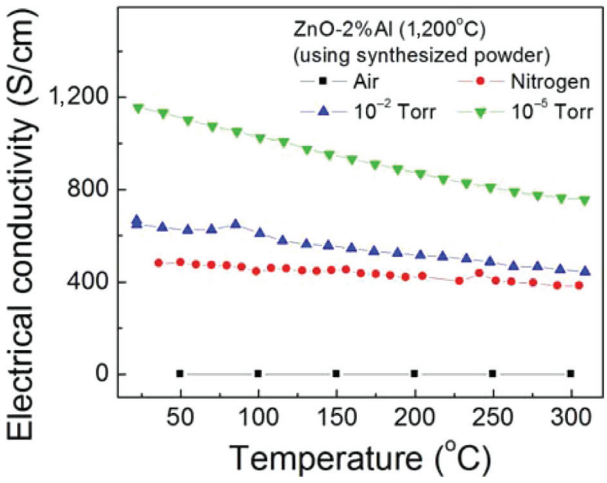

Figure 4: Electrical conductivity as a function of measurement temperature for CS-ZnO-2%Al sintered at 1,200°C under different atmospheres.

Torr) exhibited even higher σ on the order of 660 and 1,150 S/cm at room temperature that decreased to 450 and 750 S/cm, respectively, at 300°C. According to Hall measurements, samples sintered under 1.33×10^{-3} Pa vacuum had a higher carrier concentration at room temperature 1.08×10^{20} cm^{-3} compared to CS-ZnO-2%Al under 1.33 Pa (4.93×10^{19} cm^{-3}) and nitrogen (1.77×10^{19} cm^{-3}).

The sintering atmosphere as well as the initial powder condition is important for the completion of the sintering process and final defect chemistry. As mentioned earlier, the sintering mechanism of ZnO involves the diffusion of Zn ions (Norris et al. 2007; Gupta et al., 1968; Lee and Parravano 1959), resulting in high defect concentration at the surface. When sintered in air, oxygen is sufficiently available to react with Zn on the surface resulting in Zn vacancies. Zn vacancies have been proven to be electron compensating centers that have lowest formation energy of all of the possible native defects in *n*-type ZnO (Willander et al. 2010; Wang et al. 2009). On the other hand, interstitial Zn atoms function as electron donors and are formed through the reaction (Takata, Tsubone, and Yanagida 1975):

$$ZnO = Zn_i^{\times} + 1/2O_2(g) \quad [3]$$

High oxygen partial pressure impedes reaction [3] leading to a smaller amount of interstitial Zn. The oxygen in atmosphere also assists with the formation of the secondary-phase $ZnAl_2O_4$, which lowers the availability of Al as dopant. According to a prior study (Takata, Tsubone, and Yanagida 1975), chemisorbed oxygen should be taken into account to explain the electrical property change. Chemisorbed oxygen is found to provide electrons at

low temperatures, which would be hindered in air (Takata, Tsubone, and Yanagida 1975):

$$O^-_{ads} = 1/2O_2(g) + e' \quad [4]$$

All of the above factors give rise to a lower electrical conductivity of ZnO-2%Al sintered under air. On the contrary, the absence of oxygen has the following effects: (1) it assists interstitial Zn formation and increases the carrier concentration; (2) it impedes the second-phase formation and improves the Al incorporation in the ZnO matrix and (3) it increases the amount of electrons with the release mechanism of adsorbed oxygen (O^-_{ads}) at the surface of ZnO (Takata, Tsubone, and Yanagida 1975). We anticipate that vapor transport mechanism is dominant during sintering under vacuum conditions. During sintering, Zn_xO_y gas was supposed to be formed in the vacuum tube at high temperature (≥900°C) and deposited on the inside walls during cooling. The elemental analysis (Supporting Information, Figure S1 and Table S1) on the particles deposited on the wall of quartz tube revealed that there was higher oxygen concentration compared to zinc, which indicates interstitial Zn formation.

To clarify the influence of vacuum sintering and the chemical synthesis process on Al doping, different Al amounts were used in the sol–gel synthesis. This group of three pellets with different Al amounts was sintered at 1,200°C, under 1.33 Pa (10^{-2} Torr). The electrical conductivity of CS-ZnO with 1–3 mol% Al as a function of temperature is shown in Figure 5 and these results show that

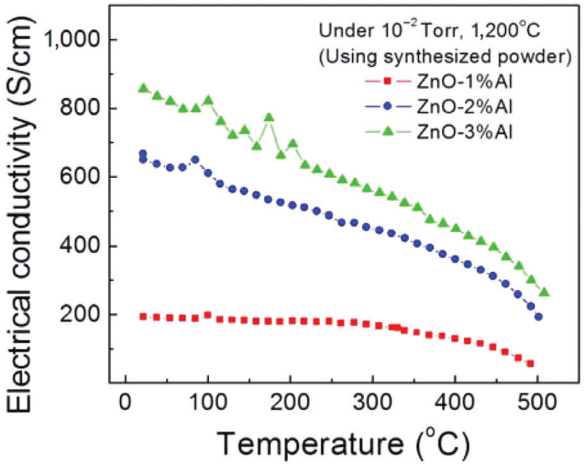

Figure 5: Electrical conductivity as a function of measurement temperature for CS-ZnO-Al (with Al in the range of 1–3 mol%) sintered at 1,200°C under pressure of 1.33 Pa (10^{-2} Torr), showing increasing electrical conductivity with increasing percentage of Al.

greater Al percentage resulted in a larger electrical conductivity. At room temperature (RT), the σ of ZnO-2%Al (666 S/cm) and ZnO-3%Al (857 S/cm) was 3.5 and 4.5 times higher than that of ZnO-1%Al (194 S/cm). The σ of all samples decreased with increasing temperature, which could be explained by stronger carrier scattering at higher temperature when electron concentration is relative high. At 500°C, the σ of ZnO-2%Al (223 S/cm) and ZnO-3%Al (301 S/cm) was 4 and 5.4 times higher than that of ZnO-1%Al (56 S/cm). According to Hall measurements, ZnO-3%Al had a carrier density of 7.11×10^{19} cm^{-3} which is larger than carrier density of 4.93×10^{19} cm^{-3} for the ZnO-2%Al. These results directly reflect the effect of vacuum sintering and Al concentration.

As a comparison (Supporting Information Figure S2), the electrical conductivity of ZnO-Al sintered under air increased from 0 to 1 mol% Al (5 S/cm at RT) and then decreased back to 3 S/cm at RT for 2 mol% Al, which indicates that the electrical conductivity exhibits peak behavior. This trend is similar to the result reported in a prior study that adding 0.25 at.% Al leads to more than a factor of 100 improvement in room temperature electrical conductivity (about 350 S/m) compared to pure ZnO, but further Al addition sharply decreases the room temperature electrical conductivity to 1 S/m when sintered in air (Jood et al. 2011). Al in excess of 0.25 at.% does not help in increasing the carrier concentration. In this prior study, samples were pressed using ZnO-Al nanopowders synthesized by chemical process under microwave irradiation. Adding additional Al would not enhance the electrical conductivity when the sintering was conducted in air. According to the phase diagram of Al_2O_3-ZnO, the solubility of Al in ZnO is limited in air (~0.3 at.% at 1,400°C) and at lower temperatures, such as 1,200°C, the solubility is even lower. However, under vacuum conditions, a greater concentration of Al can be incorporated into ZnO as shown in Figure 5.

The initial powder mixture is another factor resulting in electrical behavior variation. Comparing Figures 2 and 4, it is clear that ZnO-2%Al sintered at 1,400°C using chemically synthesized powders has electrical conductivity ten times greater than ZnO-2%Al sintered at 1,200°C using ball-milled powders of ZnO and Al_2O_3, both of which were sintered in nitrogen. When both types of samples (BM and CS) were sintered at the same sintering temperature of 1,400°C under nitrogen, CS-ZnO-2%Al had electrical conductivity 30 times greater than that of BM-ZnO-2%Al (Figure 6). From this result, it can be concluded that using sol–gel-based chemical synthesis process to prepare nanopowders improves the electrical conductivity of sintered ZnO-Al.

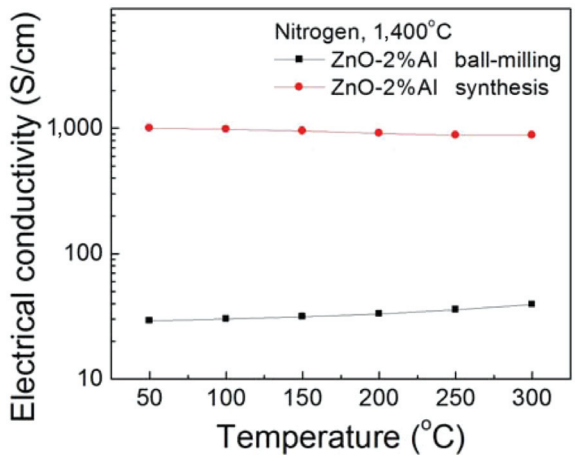

Figure 6: Electrical conductivity as a function of measurement temperature for CS- and BM-ZnO-2%Al.

The uniform distribution of Al atoms in ZnO nanopowders and lattice imperfection could be two important factors in improving the electrical conductivity. The increased Al substitution in ZnO avoids the diffusion barrier from Al_2O_3 into the ZnO matrix. The precipitation of $ZnAl_2O_4$ happens through the Al aggregation. Moreover, when the calcination of ZnO nanopowder is conducted under nitrogen the lack of oxygen causes an increase in interstitial Zn (Takata, Tsubone, and Yanagida 1975). In ball-milled powders, the Al stays in Al_2O_3 powders even when it is well mixed with ZnO. The doping process happens through reaction [1], and Al needs to diffuse through the interface of ZnO and Al_2O_3. To prove the different Al configuration and relevant particle size in two types of powders prepared by ball-milling and chemical synthesis, we examined the BM- and CS-ZnO-Al nanopowders using XRD, SEM and absorbance spectra as shown in Figure S3 and Figure 7. The XRD patterns show that both powders are rich in the zinc oxide phase. The XRD reflections of CS-ZnO-Al nanopowders are broader, implying low crystallization and imperfect lattices. Through SEM images and particle size analysis, both powders were found to have uniform size of 80 nm. So there is no significant difference in surface ratio of the two kinds of powders.

Figure 7 displays the absorbance spectra of these two types of powders (BM and CS) with different Al additions. The absorbance spectra of ball-milled ZnO-Al powders shows negligible changes with increasing Al amount. This result indicates that the structure of ball-milled ZnO-Al powders is almost the same as that of pure ZnO and Al does not substitute in the ZnO lattice. In the case of sol–gel chemical synthesis, the absorbance curves form reflections at higher wavelengths. The reflections are more obvious with increasing Al concentration. During the chemical synthesis process, Al^{3+} ions mix with Zn^{2+} ions. Al atoms stay in the ZnO matrix and modify the ZnO absorbance behavior, especially at high wavelengths (Qu 1993). The absorbance increases from ZnO without Al to ZnO-2%Al and then has a slight decrease for ZnO-3%Al. It is possible that a small amount of $ZnAl_2O_4$, which has high opacity in the long wavelength range, has formed in the ZnO-3%Al powders during calcination.

Figure 8(a) shows the Seebeck coefficient (α) of CS-ZnO-2%Al sintered under different atmospheres. All the ZnO samples exhibited negative Seebeck coefficients over the entire temperature range indicating *n*-type conduction. The value of α at room temperature was found to be −75 μV/K for CS-ZnO-2%Al sintered under nitrogen, which increased to −100 μV/K at 300°C. The value of α for CS-ZnO-2%Al under vacuum was found to be around −60 to −80 μV/K. The decrease of Seebeck coefficient value is probably because of the increase of carrier concentration. The power factor (Figure 8(b)) of ZnO samples

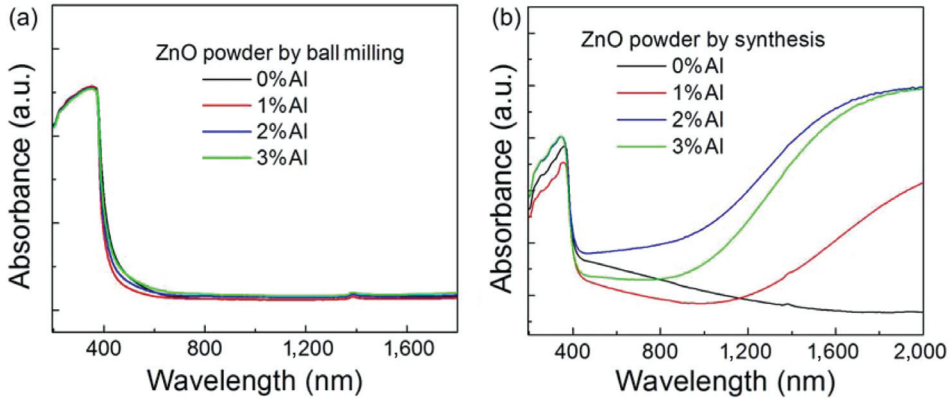

Figure 7: UV-VIS-NIR spectra of ZnO-*x*%Al ($x = 0, 1, 2, 3$) compared by (a) ball milling and (b) chemical synthesis.

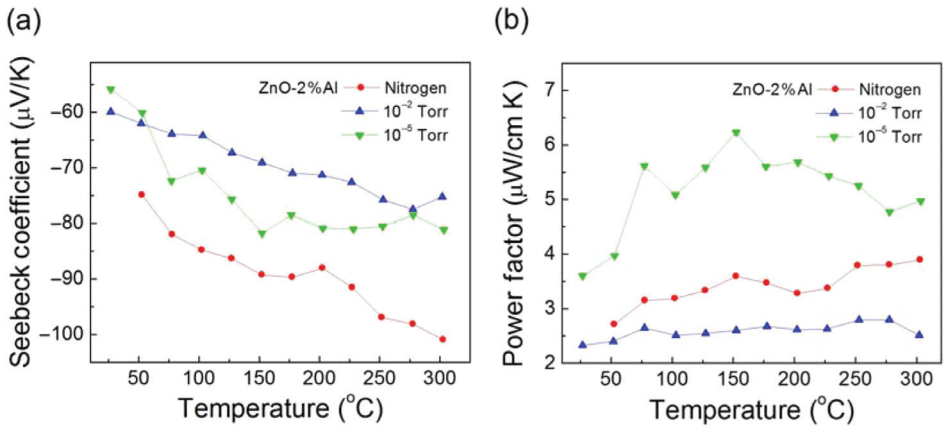

Figure 8: Seebeck coefficient and power factor as a function of measurement temperature for CS-ZnO-2%Al sintered at 1,200°C under different atmospheres.

under nitrogen and vacuum is larger than 2 μW/cm K^2, which is higher than the result of a recent paper at the same operation temperature (Jood et al. 2011).

Summary

We investigated the effect of sintering atmosphere and initial powder state on the electrical conductivity of Al-doped ZnO. Under different sintering atmospheres, ZnO-Al samples exhibited a large difference in electrical conductivity. BM-ZnO-2%Al samples showed an order of magnitude greater electrical conductivity when sintered under nitrogen as compared to air. Samples prepared using sol–gel-synthesized powders sintered under vacuum and nitrogen showed 10^7 times higher electrical conductivity than the samples sintered under air. The electrical conductivity of ZnO-2%Al sintered in vacuum at 1,200°C was found to reach 1,000 S/cm, which is typical for thermoelectric alloys. The results showed that low oxygen pressure promotes Al substitution in ZnO and impedes the formation of Zn^{2+} vacancies, leading to an increase in the amount of interstitial Zn and thereby electrical conductivity.

Acknowledgments: S.P. acknowledges the support from Institute for Critical Technologies and Applied Sciences (ICTAS).

Funding: This material was based upon the work supported by the National Science Foundation and Department of Energy through the NSF/DOE Joint Thermoelectric Partnership, Grant No. CBET-1048708.

Spplemental data

Supplemental data for this article can be accessed here.

References

Bérardan, D., C. Byl, and N. Dragoe. 2010. "Influence of the Preparation Conditions on the Thermoelectric Properties of Al-Doped ZnO." *Journal of the American Ceramic Society* 93:2352.

Cai, K. F., E. Müller, C. Drašar, and A. Mrotzek. 2003. "Preparation and Thermoelectric Properties of Al-Doped ZnO Ceramics." *Materials Science and Engineering: B* 104:45.

Gupta, T. K., and R. L. Coble. 1968. "Sintering of ZnO I Densification and Grain Growth." *Journal of the American Ceramic Society* 51:521.

Han, J. P., P. Q. Mantas, and A. M. R. Senos. 2001. "Effect of Al and Mn Doping on the Electrical Conductivity of ZnO." *Journal of the European Ceramic Society* 21:1883.

Jood, P., R. J. Mehta, Y. Zhang, G. Peleckis, X. Wang, R. W. Siegel, T. Borca-Tasciuc, S. X. Dou, and G. Ramanath. 2011. "Al-Doped Zinc Oxide Nanocomposites with Enhanced Thermoelectric Properties." *Nano Letters* 11:4337.

Joos, P., and G. Serrien. 1991. "The Principle of Braun-Le Chatelier at Surfaces." *Journal of Colloid and Interface Science* 145:291.

Lee, V. J., and G. Parravano. 1959. "Sintering Reactions of Zinc Oxide." *Journal of Applied Physics* 30:1735.

Norris, L. F., and G. Parravano. 1963. "Sintering of Zinc Oxide." *Journal of the American Ceramic Society* 46:449.

Ohtaki, M., T. Tsubota, K. Eguchi, and H. Arai. 1996. "High-Temperature Thermoelectric Properties of $(Zn_{1-x}Al_x)O$." *Journal of Applied Physics* 79:1816.

Ong, K. P., D. J. Singh, and P. Wu. 2011. "Analysis of the Thermoelectric Properties of n-Type ZnO." *Physical Review B* 83:115110.

Özgür, U., Y. I. Alivov, C. Liu, A. Teke, M. A. Reshchikov, S. Doğan, V. Avrutin, S. J. Cho, and H. Morkoç. 2005. "A Comprehensive Review of ZnO Materials and Devices." *Journal of Applied Physics* 98:041301.

Qu, Y. 1993. "Electrical and Optical Properties of Ion Beam Sputtered ZnO: Al Films as a Function of Film Thickness." *Journal of Vacuum Science & Technology A: Vacuum, Surfaces, and Films* 11:996.

Shirouzu, K., T. Ohkusa, M. Hotta, N. Enomoto, and J. Hojo. 2007. "Distribution and Solubility Limit of Al in Al_2O_3-Doped ZnO Sintered Body." *Journal of the Ceramic Society of Japan* 115:254.

Singh, A. V. 2004. "Doping Mechanism in Aluminum Doped Zinc Oxide Films." *Journal of Applied Physics* 95:3640.

Takata, M., D. Tsubone, and H. Yanagida. 1975. "Dependence of Electrical Conductivity of ZnO on Degree of Sintering." *Journal of the American Ceramic Society* 59:4.

Tsubota, T., M. Ohtaki, K. Eguchi, and H. Arai. 1997. "Thermoelectric Properties of Al-Doped ZnO as a Promising Oxide Material for High-Temperature Thermoelectric Conversion." *Journal of Materials Chemistry* 7:85.

Wang, X. J., L. S. Vlasenko, S. J. Pearton, W. M. Chen, and I. A. Buyanova. 2009. "Oxygen and Zinc Vacancies in As-Grown ZnO Single Crystals." *Journal of Physics D: Applied Physics* 42:175411.

Willander, M., O. Nur, J. R. Sadaf, M. I. Qadir, S. Zaman, A. Zainelabdin, N. Bano, and I. Hussain. 2010. "Luminescence from Zinc Oxide Nanostructures and Polymers and Their Hybrid Devices." *Materials* 3:2643.

Zhan, Z., J. Zhang, Q. Zheng, D. Pan, J. Huang, F. Huang, and Z. Lin. 2011. "Strategy for Preparing Al-Doped ZnO Thin Film with High Mobility and High Stability." *Crystal Growth & Design* 11:21.

Zhao, Y., B. Chen, A. Miner, and S. Priya. 2014. "Low Thermal Conductivity of Al-Doped ZnO with Layered and Correlated Grains." *RSC Advances* 4:18370.

Zhao, Y., A. Kumar, G. A. Khodaparast, A. Eltahir, H. Wang, and S. Priya. 2014. "Sintering Temperature-Dependent Chemical Defects and the Effect on the Electrical Resistivity of Thermoelectric ZnO." *Energy Harvesting and Systems* 1:113.

Zhao, Y., Y. K. Yan, A. Kumar, H. Wang, W. D. Porter, and S. Priya. 2012. "Thermal Conductivity of Self-Assembled Nano-Structured ZnO Bulk Ceramics." *Journal of Applied Physics* 112:034313.